Supporting Information for

Health Implications of Wintertime Fine Particulate Matter from Southwestern China

Jinyitao Wang[a,1], Fang Zhou[a,1], Wei Zhang[a], Xinquan Zhao[b], Steven J. Campbell[c], Li Zhou[d], Jialiang Feng[a], Qingyan Fu[e], Arthur W.H. Chan[f], Fumo Yang[d], Mi Tian[b,*], Shunyao Wang[a,*]

[a] School of Environmental and Chemical Engineering, Shanghai University, Shanghai, 200444, China

[b] Key Laboratory of Three Gorges Reservoir Region's Eco-Environment, Ministry of Education, Chongqing University, Chongqing, 400044, China

[c] MRC Centre for Environment and Health, Environmental Research Group, Imperial College London, 86 Wood Lane, London W12 0BZ, United Kingdom

[d] National Engineering Research Center for Flue Gas Desulfurization, Department of Environmental Science and Engineering, Sichuan University, Chengdu, 610065, China

[e] Shanghai Academy of Environmental Sciences, Shanghai 200233, China

[f] Department of Chemical Engineering and Applied Chemistry, University of Toronto, Toronto, Ontario M5S 3E5, Canada

[1] These authors contributed equally to this work.

Correspondence to

Mi Tian

tianmi628@cqu.edu.cn

Shunyao Wang

syw@shu.edu.cn

This file includes

Number of pages: 28

Number of Table: 5

Number of Figures: 10

Supplemental Text

S1. Analysis by ion chromatography

For the analysis of water-soluble inorganic ions, a quarter of each quartz filter was first extracted using ultrapure water in an ultrasonic bath for 30 min, and then filtered through a syringe filter (0.45 μm pore size). Both anions (SO_4^{2-}, NO_3^- and Cl^-) and cations (Na^+, NH_4^+, K^+, Mg^{2+} and Ca^{2+}) were determined using ion chromatograph (Dionex, Dionex 600, USA). Anions were separated using an AS11-HC column with 30 mM KOH as an eluent at a flow rate of 1.0 mL min^{-1}. Cations were determined using a CS12A column with 20 mM MSA (methanesulfonic acid) at a flow rate of 1.0 mL min^{-1}. Individual standard solutions of all investigated ions (1000 mg L^{-1}) were diluted in series to construct the calibration curves. The correlation coefficients of the linear regression of the standard curves were all above 0.999. Field blanks were prepared and analyzed together with the samples, and then subtracted from the samples. The concentrations of water-soluble inorganic ions in field blanks were in the range of 0.008–0.13 μg m^{-3}. The relative standard deviation of each ion was measured to be within 8% for all replicates.

S2. OC/EC measurement

Organic carbon (OC) and elemental carbon (EC) were analyzed using a multi-wavelength Carbon Analyzer (Model 2015, DRI, USA) in accordance with the Interagency Monitoring of Protected Visual Environment (IMPROVE-A) protocol [1-3]. Four OC fractions (i.e. OC_1, OC_2, OC_3, and OC_4) were measured at the temperature of 140 °C, 280 °C, 480 °C, and 580 °C, respectively, in a helium buffer gas. During each run, three EC fractions (i.e. EC_1, EC_2, and EC_3) were measured at the temperature of 580 °C, 740 °C, and 840 °C, respectively.

S3. Health risk of metallic elements

Hazard quotient (HQ) is used to measure the non-carcinogenic health risks of heavy metals in ambient PM (Eqn.S1). ADD represents the average daily exposure dose of heavy metals through different exposure pathways (mg kg^{-1}day^{-1}). Detailed formulas and parameterization of ADD calculation regarding the three different exposure pathways (ingestion, inhalation, and dermal contact) can be found in Text S3. Based on the calculated ADD, HQ can be calculated by dividing the ADD by the specific reference dose (RfD). The reference dose values (Table S3) used in this study are based on previous literature [34, 35].

$$HQ = \frac{ADD}{RfD} \qquad \text{(S1)}$$

Note that the reference dose is an approximation of maximum risk through daily exposure taken into account during the lifetime [34]. If HQ < 1 (the average daily dose is less than the reference dose), it means that the adverse health effects are negligible. Otherwise, if HQ > 1 (the average daily dose is greater than the reference dose), the specific exposure pathway may have significant adverse effects on human health [37].

Excess cancer risk (ECR) can be estimated as the incremental probability that an individual develops cancer over a lifetime due to total exposure to potential carcinogens, which can be calculated using Eqn.S2 [33].

$$ECR = \frac{C \times ET \times EF \times ED \times IUR}{AT} \qquad \text{(S2)}$$

Where C is the pollutant concentration (μg m^{-3}); ET is the exposure time (8 hours day^{-1}); EF is the exposure frequency (180 days $year^{-1}$); ED is the duration of exposure, which in this study was 24 years (adults) and 6 years (children) in this study; IUR is the inhalation unit risk (μg $m^{-3})^{-1}$; AT is the average exposure time of the specific carcinogen (70 years × 365 days $year^{-1}$ × 24 hours day^{-1}). It should be noted that only the carcinogenic risk of metals via inhalation was considered in this study.

Average daily exposure dose of heavy metals through ingestion (ADD_{ing}, mg $kg^{-1}day^{-1}$)

$$ADD_{ing} = \frac{C \times IngR \times EF \times ED \times CF}{BW \times AT} \qquad \text{(S3)}$$

Average daily exposure dose of heavy metals through inhalation (ADD_{inh}, mg $kg^{-1}day^{-1}$)

$$ADD_{inh} = \frac{C \times IngR \times EF \times ED}{BW \times AT \times PEF} \qquad \text{(S4)}$$

Average daily exposure dose of heavy metals through dermal contact (ADD_{derm}, mg $kg^{-1}day^{-1}$)

$$ADD_{derm} = \frac{C \times SA \times AF \times EV \times ABS \times EF \times ED \times CF}{BW \times AT} \tag{S5}$$

Where C is the concentration of metal in PM (mg kg^{-1}); IngR is the intake rate (mg day^{-1}), which was 30 mg day^{-1} for adults and 60 mg day^{-1} for children in this study. InhR is the inhalation rate (m^3 day^{-1}), which in this study was 7.63 (adults) and 20 (children); EF is the exposure frequency, 180 days $year^{-1}$ in this study; ED is the duration of exposure, which in this study was 24 years (adults) and 6 years (children); BW is body weight. In this study, adults were 70 kg and children were 15 kg. SA is the skin surface area parameter, in this study, adults 5700 cm^2 and children 2800 cm^2; AF is the adhesion factor of soil to skin, which in this study was 0.07 mg cm^{-2} $event^{-1}$ (adults) and 0.2 mg cm^{-2} $event^{-1}$ (children). EV is the event frequency, which is 1 event day^{-1}; ABS is skin absorption fraction 0.001 in this study; PEF is the particle emission factor of 1.36×10^9 m^3 kg^{-1}. The average time of non-carcinogens AT was ED × 365 days $year^{-1}$ in this study; CF is a conversion factor of about 10^{-6} kg mg^{-1}. All the parameters used in the calculation can be found in EPA report [4]. Reference concentration values (RfC, mg m^{-3}) and inhalation unit risks (IUR, μg^{-1} m^3) were used to calculate the hazard quotient (HQ) and excess carcinogenic risk [5, 6].

As illustrated in Figure S4a, the HQ values of Chongqing wintertime $PM_{2.5}$ for adults were found to be higher than those estimated for children. Most of the HQ values are less than 1, while HQ_{As} and HQ_{Pb} are greater than 1. Previous work has pointed out that the non-carcinogenic risk of heavy metals should not be considered as negligible when HQ > 1 [7]. Therefore, the levels of As and Pb in Chongqing $PM_{2.5}$ may cause significant non-carcinogenic adverse effects. Among different exposure pathways, dermal (HQ_{der}) caused non-cancer risk was found to be the lowest (less than 1) while ingestion (HQ_{ing}) and inhalation (HQ_{inh}) caused non-cancer risk exceeded 1 for Cr, As, and Pb. Attentions should also be given that the HQ_{inh} of $PM_{2.5}$ in wintertime Chongqing (5.90 for adults and 11.58 for children) was higher than those reported in other cities on the East coast of China, such as Guangzhou (1.04-1.16 for adults, 1.93-2.15 for children), Hangzhou (2.41 for adults, 1.32-1.43 for children), Shanghai (1.05-1.21 for adults, 1.95-2.25 for children), and Beijing (1.02-1.19 for adults, 1.9-2.2 for children). The HQ_{inh} value estimated for Chongqing in this study was more similar to the less developed cities located on the central west part of the country, such as Xi'an (7.24-7.84 for adults, 13.4-14.5 for children) and Kunming (6.91-7.11 for adults, 12.8-13.2 for children) [7].

Cr, As, Pb, Cd are known carcinogenic metals in PM [7]. According to Figure S4b, the ECR of carcinogenic metal elements follows As > Cr (VI) > Cd > Pb. Cr and As are mainly derived from coal combustion [8]. It should be noted that nearly 80% coal resources of the whole country is distributed in the west region [7], explaining that Cr (VI) and As emerged as the two heavy metals with the highest excessive carcinogenic risk in Chongqing. Overall, the observed ECR values for metallic composition in Chongqing are comparable with those observed in other Asian countries. For example, the ECR values of Cd, Cr (VI), and Cd in $PM_{2.5}$ collected Indian were 1.90×10^{-6}, 1.01×10^{-4}, and 0.40×10^{-6} [9]. In Ulsan from South Korea, the ECR values for Cd and Cr (VI) were reported to be 8.7×10^{-6} and 1.74×10^{-5}, respectively [10]. More efforts should be paid in the future for regulating metallic airborne pollution in the southwestern area of China.

S4. Multilinear regression results

The unstandardized regressions with different independent variables were shown as following. The first equation in each group in italics is the regression included in the main text of the paper (S4, S15, S39).

For OP_v^{DTT},

$$\mathit{OP_v^{DTT}=0.10OC + 7.14Cu + 1.69Zn + 1.79PAHs + 8.67OPAHs+0.52} \qquad r^2=0.84 \quad (S4)$$

$$OP_v^{DTT} = 0.53PAHs + 14.58Cu + 0.097 \qquad r^2=0.62 \quad (S5)$$

OP_v^{DTT}=0.47OPAHs + 16. 68Cu + 0.084 r^2=0.61 (S6)

OP_v^{DTT}=9.84NPAHs + 1. 57Cu + 0.006 r^2=0.62 (S7)

OP_v^{DTT}=0.25EC + 60. 41Cu + 0.89 r^2=0.73 (S8)

OP_v^{DTT}=0.23EC + 5.66Cu + 5.56Zn + 0.11PAHs + 5.77OPAHs r^2= 0.76 (S9)

OP_v^{DTT}=0.096OC + 18.57Mn + 0.56 r^2= 0.86 (S10)

OP_v^{DTT}=0.99OC + 21.58Fe + 4.74 r^2= 0.86 (S11)

OP_v^{DTT}=0.25EC + 2.40Fe + 0.79 r^2= 0.78 (S12)

OP_v^{DTT}=0.108OC + 14.99OPAHs + 0.482 r^2= 0.84 (S13)

OP_v^{DTT}=0.25EC + 6.72Zn + 0.79 r^2= 0.76 (S14)

For OP_v^{EPR},

OP_v^{EPR}=0.001EC + 0.007Fe + 0.088Cu -0.63PAHs +14.63NPAHs -0.001

r^2=0.73 (S15)

OP_v^{EPR}=10.2NPAHs + 0.44Cu + 0.01 r^2=0.59 (S16)

OP_v^{EPR}=0.17OPAHs -0.4PAHs+ 3.88Cu + 0.41Mn +0.02 r^2=0.62 (S17)

OP_v^{EPR}= 0.0003OC + 13.301NPAHs r^2=0.70 (S18)

OP_v^{EPR}= 0.0003OC + 0.317Cu r^2=0.60 (S19)

OP_v^{EPR}= 0.0004OC + 0.511Cu – 0.036Zn r^2=0.65 (S20)

For *in vitro ROS_V*,

in vitro ROS_V= 1.19Fe+ 99.52Cu + 807.84NPAH -47.17Cd- 74.57Ti+0.36

r^2=0.68 (S21)

in vitro $ROS_V = 0.15EC + 169.33NPAH + 3.38Zn - 14.61Pb + 0.19$

$r^2=0.54$ (S22)

in vitro $ROS_V = 86.91NPAH + 11.09Cu - 4.29Cd - 5.22Ti + 0.028$

$r^2=0.67$ (S23)

in vitro $ROS_V = 0.018EC + 174.45NPAH + 0.34Zn + 32.04As - 49.94Cd - 22.12Pb + 0.023$

$r^2=0.67$ (S24)

in vitro $ROS_V = 0.19EC + 185.76NPAH + 3.54Zn - 53.01Cd - 18.12Pb + 0.21$

$r^2=0.61$ (S25)

in vitro $ROS_V = 8.68OPAH + 0.11EC - 46.09Cd + 0.45$ $r^2=0.50$ (S26)

in vitro $ROS_V = 0.98EC + 79.21OPAH + 4.64$ $r^2=0.44$ (S27)

The standardized regressions with different independent variables were shown as following. The first equation in each group in italics is the regression included in the main text (S21, S32).

For OP_v^{DTT},

$OP_v^{DTT}=0.697OC + 0.033Cu + 0.081Zn + 0.63PAHs + 0.141OPAHs$

$r^2=0.84$ (S28)

$OP_v^{DTT}=0.18PAHs + 0.63Cu - 1.4988E\text{-}15$ $r^2=0.61$ (S29)

$OP_v^{DTT}=0.071OPAHs + 0.72Cu - 1.507E\text{-}15$ $r^2=0.61$ (S30)

$OP_v^{DTT}=0.15NPAHs + 0.68Cu - 1.3862E\text{-}15$ $r^2=0.62$ (S31)

$OP_v^{DTT}=0.129PAHs + 0.127NPAHs + 0.59Cu - 1.3738E\text{-}15$ $r^2=0.62$ (S32)

$OP_v^{DTT}=0.271OC + 0.065PAHs + 0.189NPAHs + 0.093Cu + 0.166Mn + 0.231Zn$

$r^2=0.71$ (S33)

$OP_v^{DTT}=0.683OC + 0.332Mn$ $r^2= 0.86$ (S34)

$OP_v^{DTT}=0.701OC + 0.317Fe$ $r^2= 0.86$ (S35)

OP_v^{DTT}=0.62EC + 0.352Fe r^2= 0.78 (S36)

OP_v^{DTT}=0.765OC + 0.243OPAHs r^2= 0.84 (S37)

OP_v^{DTT}=0.609EC + 0.325Zn r^2= 0.76 (S38)

For OP_v^{EPR},

OP_v^{EPR}=0.585EC + 0.242Fe + 0.091Cu -0.492PAHs +0.488NPAHs r^2=0.73 (S39)

OP_v^{EPR}=0.524NPAHs + 0.475EC + 0.07Cu +0.026 r^2=0.68 (S40)

OP_v^{EPR}=0.069PAHs + 0.523Fe + -8.9743E-17 r^2= 0.34 (S41)

OP_v^{EPR}=0.288EC + 0.015Mn + 0.478Cu +0.016 r^2=0.54 (S42)

OP_v^{EPR}= 0.525OC + 0.443NPAHs r^2=0.70 (S43)

OP_v^{EPR}= 0.487OC + 0.327Cu r^2=0.60 (S44)

OP_v^{EPR}= 0.631OC + 0.528Cu – 0.389Zn r^2=0.65 (S45)

For *in vitro ROS_V*,

in vitro ROS_V= 0.344Fe+ 0.903Cu + 0.235NPAH -0.250Cd- 0.753Ti

r^2=0.68 (S46)

in vitro ROS_V= 0. 750EC+ 0.493NPAH + 0.323Zn -0.701Pb

r^2=0.54 (S47)

in vitro ROS_V= 0.253NPAH + 1.007Cu -0.227Cd- 0.528Ti

r^2=0.67 (S48)

in vitro ROS_V= 0.881EC+0.507NPAH + 0.331Zn+0.312As -0.264Cd- 1.062Pb

r^2=0.67 (S49)

in vitro ROS_V= 0.924EC+0.540NPAH + 0.338Zn -0.280Cd-0.869Pb

r^2=0.61 (S50)

in vitro ROS_V= 0.275OPAH + 0.523EC -0.227Cd r^2=0.50 (S51)

in vitro ROS_V= 0.523EC +0.251OPAH r^2=0.44 (S52)

Supplemental Tables

Table S1. Comparison of OP^{DTT} values measured in this study and other studies.

Location	**Year**	OP_V^{DTT} **(nmol min^{-1} m^{-3})**	**Reference**
Chongqing	Winter, 2015–2016	2.83±1.28	This study
Wuhan	2012	1.8–8.2	[11]
Hangzhou	2017	0.62 ± 0.24	[12]
Shanghai	2016	0.19 ± 0.04	[13]
Xiamen (Siming)	2015–2018	0.632 ± 0.299	[14]
Xiamen (Xiang'an)		0.562 ± 0.247	
Guangzhou	January, 2018	0.93 ± 0.21	[15]
	April, 2018	0.89 ± 0.20	
Jinzhou	2015–2016	4.4 ± 2.6	[16]
Tianjin	2015–2016	6.8 ± 3.4	
Yantai	2015–2016	4.2 ± 2.7	
Nanjing (Xianlin)	2020–2021	2.42	[17]
Nanjing (Gulou)		1.34	
Nanjing	2019–2020	2.1 ± 1.1	[18]
Qingdao	2021–2022	2.15 ± 1.24	[19]
Xi’an	Spring, 2017	0.53 (0.19–0.85)	[20]
	Summer, 2017	0.50 (0.24–0.80)	
	Autumn, 2017	0.40 (0.24–0.74)	
	Winter, 2017	0.64 (0.43–1.10)	
Lecce	2013–2016	0.29 ± 0.12	[21]
Amsterdam	2012	0.20 ± 0.01	[22]
Frankfurt		0.28 ± 0.02	
London		0.20 ± 0.01	
Milan		0.51 ± 0.07	

Stockholm		0.22 ± 0.02	
Thessaloniki		0.41 ± 0.02	
Southern Alps		0.11 ± 0.01	
Toronto	2016–2017	0.0306 ± 0.0107	[23]
Atlanta	2012–2013	0.31	[24]

Table S2. Comparison of OP^{EPR} values measured in this study and other studies.

Location	Year	OP_{V}^{EPR} (spins m^{-3})	Reference
Chongqing	winter, 2015−2016	$3.3 \pm 1.55\times10^{13}$ (1.24-6.59×10^{13}) $1.2\times10^{-2}\pm5\times10^{-3}$ (nmol m^{-3})	This study
Wanzhou, Chongqing	2017	$7.0 \pm 1.7 \times 10^{13}$	[25]
Xi'an	Jan. −Feb., 2017	2.58–23.47×10^{14}	[26]
	spring, 2017	1.7×10^{14}	[27]
	summer, 2017	9×10^{13}	
	autumn, 2017	7×10^{13}	
	winter, 2017	2.1×10^{14}	
	2017	2.58–5.41×10^{14}	[28]
Linfen	Before lockdown, 2019	1.3×10^{13} (0.65–2.7×10^{13})	[29]
	During lockdown, 2020	1.4×10^{13} (0.62–5.2×10^{13})	
Beijing	winter, 2020	non-heating and heating: 16.2×10^{12} and 14.2×10^{12} (3.4–39.5×10^{12})	[30]
Yuncheng		non-heating and heating: 12.7×10^{12} and 28.2×10^{12} (4.8–59.2×10^{12})	
Erenhot	2016	1.6×10^{13}	[31]
Zhangbei		5.71×10^{13}	
Jinan		4.57×10^{13}	
Nanjing	2019	7.61×10^{12} (2.78×10^{12} –1.72×10^{13})	[32]
Mainz	2019	$3.6 \pm 3.1 \times 10^{12}$	[33]
Lahore, Pakistan	summer, 2019	1.78×10^{13} (2.9×10^{12}–4.6×10^{13})	[34]
	winter, 2019	1.20×10^{14} (2.9×10^{13}–2.9×10^{14})	

Table S3. Recommended values of Reference Doses (RfD) (mg kg^{-1} day^{-1}).

Heavy metal	As	Cd	Cr	Cu	Ni	Pb	V	Zn
RFD_{ing}	3.00×10^{-4}	1.00×10^{-3}	3.00×10^{-3}	4.00×10^{-2}	2.00×10^{-2}	3.50×10^{-3}	7.00×10^{-3}	3.00×10^{-1}
RFD_{inh}	3.00×10^{-4}	1.00×10^{-3}	2.86×10^{-5}	4.02×10^{-2}	3.52×10^{-3}	3.52×10^{-3}	7.00×10^{-3}	3.01×10^{-1}
RFD_{der}	1.23×10^{-4}	1.00×10^{-5}	6.00×10^{-5}	1.20×10^{-2}	5.40×10^{-3}	5.25×10^{-4}	7.00×10^{-5}	6.00×10^{-1}

RFD_{ing}: Ingestion reference dose.

RFD_{inh}: Inhalation reference dose.

RFD_{der}: Dermal contact reference dose.

Table S4. Correlation between OP_V (OP_v^{DTT}, OP_v^{EPR} and *in vitro* ROS_V) and non-metallic $PM_{2.5}$ components measured in Chongqing.

	OP_v^{DTT}	OP_v^{EPR}	ROS_V	SO_4^{2-}	NO_3^-	NH_4^+	Cl^-	K^+	OC	EC	SO_2	NO_2	O_3	CO	PAHs	NPAHs	OPAHs	CHO	CHNO	CHOS	CHNOS
OP_v^{DTT}	1	.716**	.582**	.800**	.782**	.803**	.710**	.820**	.890**	.838**	.400*	.784**	-.390*	.699**	.595**	.638**	0.168	.440*	0.189	0.118	1
OP_v^{EPR}	.716**	1	.606**	.721**	.762**	.740**	.581**	.742**	.743**	.736**	.372*	.778**	-.369*	.513**	.681**	.485**	0.039	0.084	-0.101	-0.172	.716**
ROS_V	.582**	.606**	1	.585**	.595**	.611**	.655**	.650**	.564**	.634**	0.356	.639**	-.495**	.584**	.605**	.557**	0.011	0.179	-0.050	-0.046	.582**
SO_4^{2-}	.800**	.721**	.585**	1	.952**	.990**	.680**	.957**	.942**	.890**	.408*	.881**	-0.279	.423*	.407*	0.346	-0.092	.379*	-0.059	-0.130	.800**
NO_3^-	.782**	.762**	.595**	.952**	1	.978**	.721**	.945**	.932**	.888**	.454*	.911**	-0.326	.450*	.494**	.421*	-0.051	0.261	-0.143	-0.196	.782**
NH_4^+	.803**	.740**	.611**	.990**	.978**	1	.727**	.970**	.944**	.903**	.432*	.898**	-0.306	.455*	.446*	.401*	-0.070	0.344	-0.096	-0.149	.803**
Cl^-	.710**	.581**	.655**	.680**	.721**	.727**	1	.805**	.767**	.826**	.414*	.740**	-.540**	.753**	.485**	.693**	0.090	0.269	-0.032	-0.056	.710**
K^+	.820**	.742**	.650**	.957**	.945**	.970**	.805**	1	.955**	.945**	.466*	.910**	-.435*	.560**	.493**	.515**	-0.002	0.341	-0.056	-0.102	.820**
OC	.890**	.743**	.564**	.942**	.932**	.944**	.767**	.955**	1	.937**	.482**	.901**	-.411*	.579**	.491**	.513**	0.059	.414*	0.042	-0.078	.890**
EC	.838**	.736**	.634**	.890**	.888**	.903**	.826**	.945**	.937**	1	.471**	.869**	-.562**	.673**	.528**	.599**	0.027	0.328	-0.069	-0.095	.838**
SO_2	.400*	.372*	0.356	.408*	.454*	.432*	.414*	.466*	.482**	.471**	1	.483**	-0.124	.561**	0.313	.579**	.413*	0.272	.405*	0.325	.400*
NO_2	.784**	.778**	.639**	.881**	.911**	.898**	.740**	.910**	.901**	.869**	.483**	1	-.463*	.596**	.596**	.520**	0.162	0.327	-0.003	-0.070	.784**
O_3	-.390*	-.369*	-.495**	-0.279	-0.326	-0.306	-.540**	-.435*	-.411*	-.562**	-0.124	-.463*	1	-.481**	-.518**	-.511**	-0.122	-0.089	0.035	-0.040	-.390*
CO	.699**	.513**	.584**	.423*	.450*	.455*	.753**	.560**	.579**	.673**	.561**	.596**	-.481**	1	.660**	.921**	.482**	.403*	0.345	0.349	.699**
PAHs	.595**	.681**	.605**	.407*	.494**	.446*	.485**	.493**	.491**	.528**	0.313	.596**	-.518**	.660**	1	.671**	0.251	0.233	0.138	0.189	.595**
NPAHs	.638**	.485**	.557**	0.346	.421*	.401*	.693**	.515**	.513**	.599**	.579**	.520**	-.511**	.921**	.671**	1	.566**	0.355	.398*	.428*	.638**
OPAHs	0.168	0.039	0.011	-0.092	-0.051	-0.070	0.090	-0.002	0.059	0.027	.413*	0.162	-0.122	.482**	0.251	.566**	1	0.275	.709**	.727**	0.168
CHO	.440*	0.084	0.179	.379*	0.261	0.344	0.269	0.341	.414*	0.328	0.272	0.327	-0.089	.403*	0.233	0.355	0.275	1	.571**	0.308	.440*
CHNO	0.189	-0.101	-0.050	-0.059	-0.143	-0.096	-0.032	-0.056	0.042	-0.069	.405*	-0.003	0.035	0.345	0.138	.398*	.709**	.571**	1	.801**	0.189
CHOS	0.118	-0.172	-0.046	-0.130	-0.196	-0.149	-0.056	-0.102	-0.078	-0.095	0.325	-0.070	-0.040	0.349	0.189	.428*	.727**	0.308	.801**	1	0.118
CHNOS	1	.716**	.582**	.800**	.782**	.803**	.710**	.820**	.890**	.838**	.400*	.784**	-.390*	.699**	.595**	.638**	0.168	.440*	0.189	0.118	1

**. At level 0.01, the correlation was significant. *. At level 0.05, the correlation was significant.

Table S5. Correlation between OP_V (OP_v^{DTT}, OP_v^{EPR} and *in vitro* ROS_V) and metallic $PM_{2.5}$ compositions measured in Chongqing.

	OP_v^{DTT}	OP_v^{EPR}	ROS_V	Ca	Sc	Ti	V	Cr	Mn	Fe	Co	Ni	Cu	Zn	Ga	As	Se	Br	Sr	Ba	Pb	Cd
OP_v^{DTT}	1	.716**	0.177	0.148	-.550**	.619**	0.318	0.282	.741**	.699**	-.467**	0.282	.776**	.750**	.841**	.633**	.802**	.721**	.482**	.461*	.863**	0.259
OP_v^{EPR}	.716**	1	.442*	0.231	-.479**	.569**	0.327	0.263	.606**	.581**	-0.299	0.345	.708**	.495**	.689**	.667**	.648**	.433*	0.349	0.357	.685**	0.154
ROS_V	0.177	.442*	1	0.182	-0.023	0.314	-0.013	0.227	0.218	0.231	0.016	0.294	0.201	0.133	0.174	0.249	0.223	0.013	0.034	-0.023	0.143	-0.200
Ca	0.148	0.231	0.182	1	-.537**	.693**	0.019	0.346	0.312	.434*	-0.050	0.265	0.276	0.190	0.093	0.039	0.130	0.231	.639**	0.090	0.113	0.013
Sc	-.550**	-.479**	-0.023	-.537**	1	-.639**	0.049	-0.253	-.471**	-.521**	0.114	-0.303	-.522**	-.505**	-.493**	-.414*	-.613**	-.517**	-.696**	-0.281	-.515**	0.107
Ti	.619**	.569**	0.314	.693**	-.639**	1	0.304	.649**	.860**	.923**	-0.343	.616**	.781**	.607**	.658**	.492**	.619**	.675**	.617**	0.153	.566**	0.089
V	0.318	0.327	-0.013	0.019	0.049	0.304	1	0.175	.402*	.393*	-0.139	0.166	.394*	0.154	.375*	0.299	.414*	0.222	0.015	0.079	0.325	.642**
Cr	0.282	0.263	0.227	0.346	-0.253	.649**	0.175	1	.702**	.754**	-.420*	.811**	.473**	0.351	0.344	.369*	0.197	.550**	0.252	0.078	0.254	0.091
Mn	.741**	.606**	0.218	0.312	-.471**	.860**	.402*	.702**	1	.976**	-.508**	.667**	.865**	.717**	.804**	.648**	.643**	.790**	.396*	0.258	.676**	0.184
Fe	.699**	.581**	0.231	.434*	-.521**	.923**	.393*	.754**	.976**	1	-.471**	.685**	.857**	.708**	.760**	.620**	.647**	.784**	.495**	0.254	.633**	0.178
Co	-.467**	-0.299	0.016	-0.050	0.114	-0.343	-0.139	-.420*	-.508**	-.471**	1	-.372*	-.437*	-.407*	-.414*	-.396*	-0.253	-.447*	-0.021	-0.153	-.438*	-0.060
Ni	0.282	0.345	0.294	0.265	-0.303	.616**	0.166	.811**	.667**	.685**	-.372*	1	.573**	.382*	.470**	.469**	0.349	.545**	0.268	0.027	0.345	0.031
Cu	.776**	.708**	0.201	0.276	-.522**	.781**	.394*	.473**	.865**	.857**	-.437*	.573**	1	.781**	.843**	.718**	.755**	.722**	.498**	0.348	.779**	0.214
Zn	.750**	.495**	0.133	0.190	-.505**	.607**	0.154	0.351	.717**	.708**	-.407*	.382*	.781**	1	.857**	.673**	.675**	.685**	.636**	.527**	.778**	0.146
Ga	.841**	.689**	0.174	0.093	-.493**	.658**	.375*	0.344	.804**	.760**	-.414*	.470**	.843**	.857**	1	.816**	.816**	.743**	.478**	0.330	.917**	0.251
As	.633**	.667**	0.249	0.039	-.414*	.492**	0.299	.369*	.648**	.620**	-.396*	.469**	.718**	.673**	.816**	1	.703**	.648**	0.311	0.249	.782**	0.097
Se	.802**	.648**	0.223	0.130	-.613**	.619**	.414*	0.197	.643**	.647**	-0.253	0.349	.755**	.675**	.816**	.703**	1	.632**	.479**	0.244	.760**	0.213
Br	.721**	.433*	0.013	0.231	-.517**	.675**	0.222	.550**	.790**	.784**	-.447*	.545**	.722**	.685**	.743**	.648**	.632**	1	.418*	0.195	.648**	0.280
Sr	.482**	0.349	0.034	.639**	-.696**	.617**	0.015	0.252	.396*	.495**	-0.021	0.268	.498**	.636**	.478**	0.311	.479**	.418*	1	.583**	.526**	0.145
Ba	.461*	0.357	-0.023	0.090	-0.281	0.153	0.079	0.078	0.258	0.254	-0.153	0.027	0.348	.527**	0.330	0.249	0.244	0.195	.583**	1	.445*	0.139
Pb	.863**	.685**	0.143	0.113	-.515**	.566**	0.325	0.254	.676**	.633**	-.438*	0.345	.779**	.778**	.917**	.782**	.760**	.648**	.526**	.445*	1	0.232
Cd	0.259	0.154	-0.200	0.013	0.107	0.089	.642**	0.091	0.184	0.178	-0.060	0.031	0.214	0.146	0.251	0.097	0.213	0.280	0.145	0.139	0.232	1

****. At level 0.01, the correlation was significant. *. At level 0.05, the correlation was significant.**

Supplemental Figures

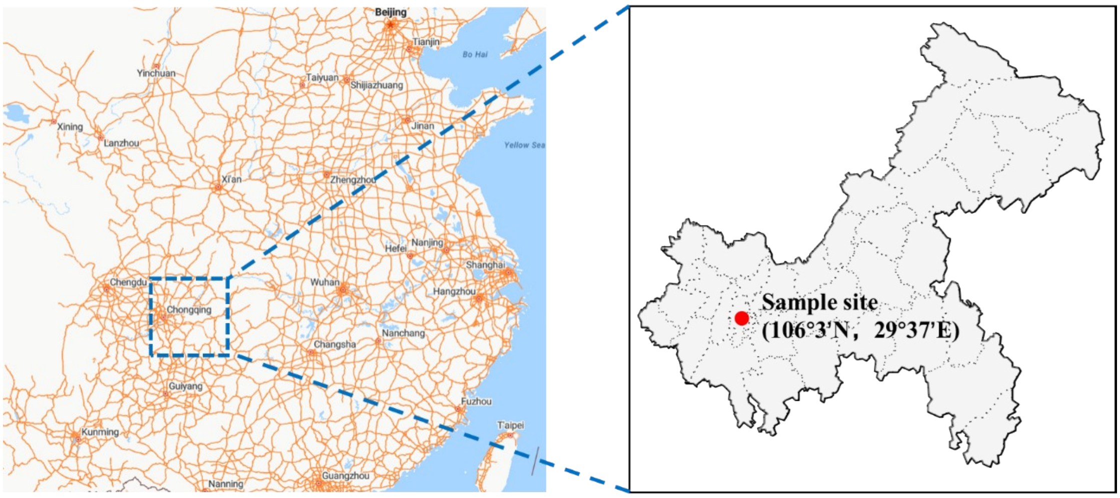

Figure S1. Geographical schematic of the sampling site (106°3′N, 29°37′E) in Chongqing.

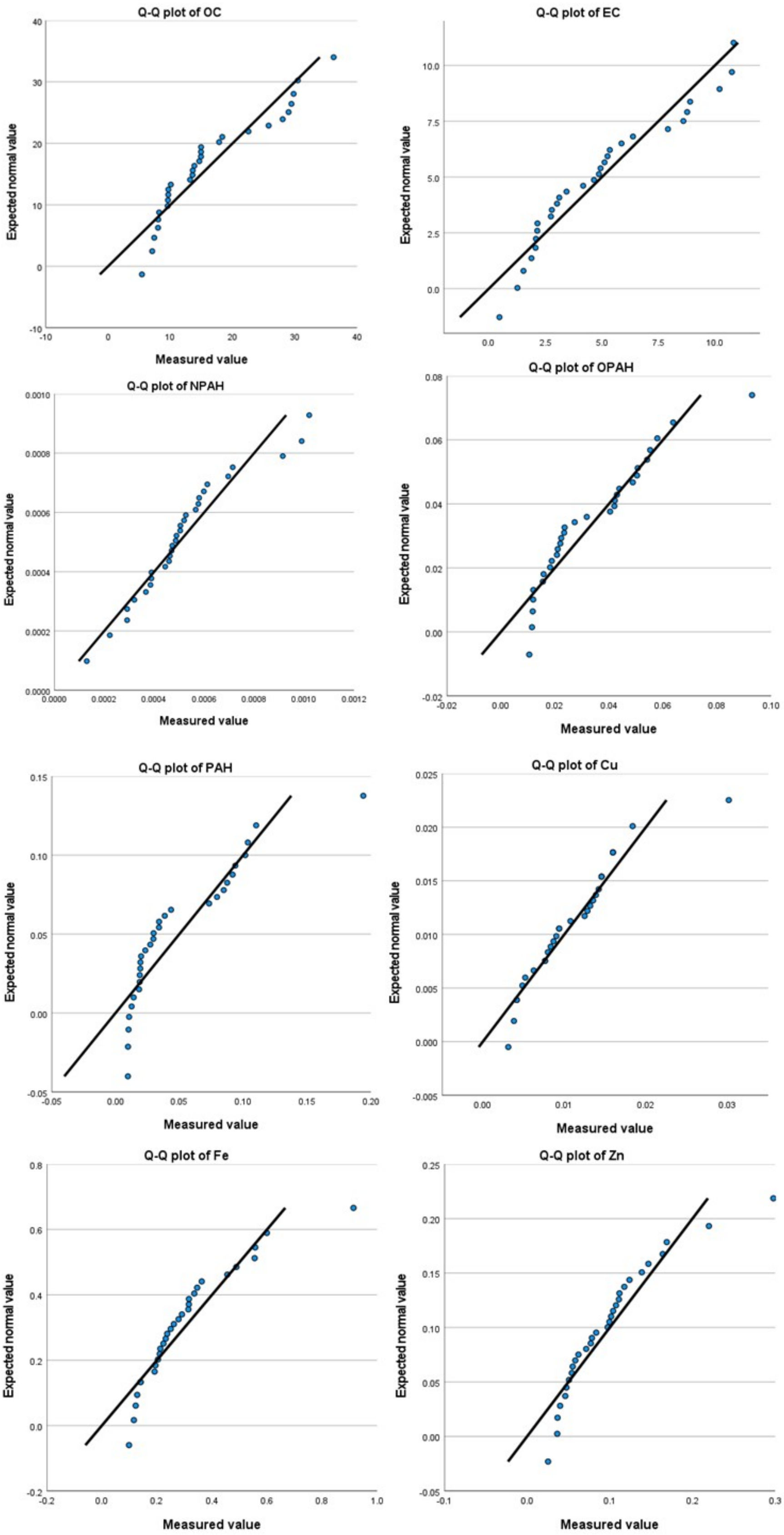

Figure S2. The residual plots (Q-Q plots) of the partial components of $PM_{2.5}$ in Chongqing.

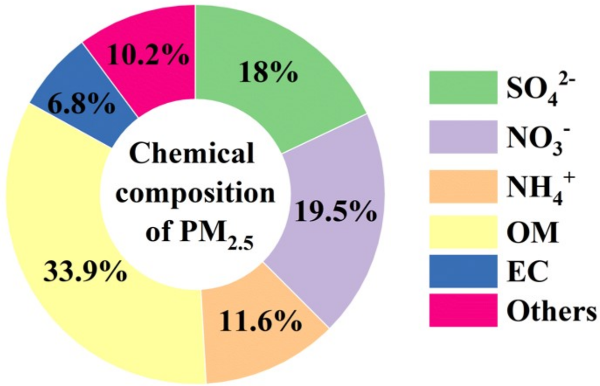

Figure S3. Chemical composition of $PM_{2.5}$ in wintertime Chongqing.

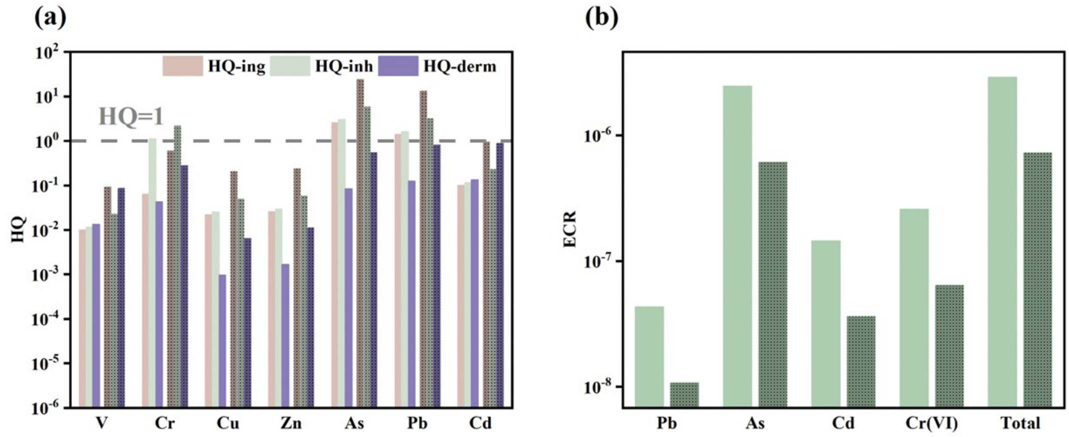

Figure S4. (a) HQ for adults (light color) and children (dark color) upon metal exposure (V, Cr, Cu, Zn, As, Pb, Cd) via ingestion (HQ-ing), inhalation (HQ-inh), and dermal (HQ-derm) exposure pathways. (b) ECRs of metals (Cr, As, Pb, and Cd) for adults (light color) and children (dark color) in $PM_{2.5}$ collected during wintertime Chongqing.

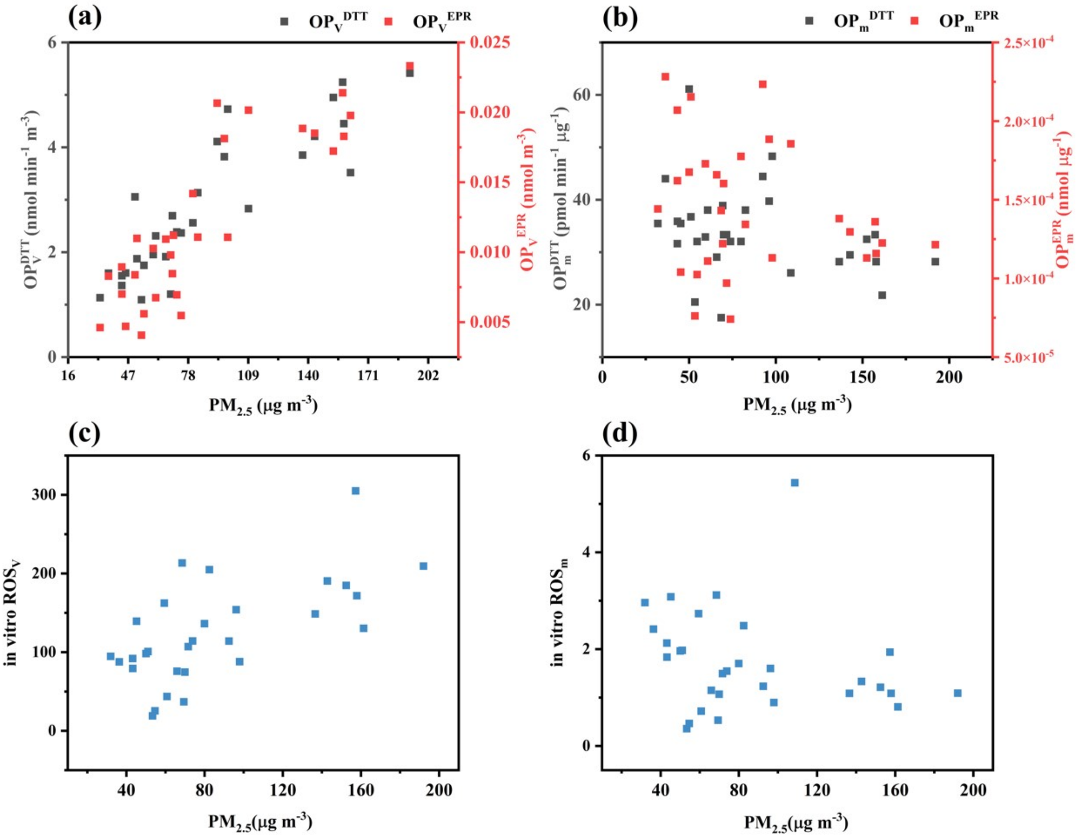

Figure S5. Correlation between (a) OP_v , (b) *in vitro* ROS_V, (c) OP_m and (d) *in vitro* ROS_m with $PM_{2.5}$ mass concentration, respectively.

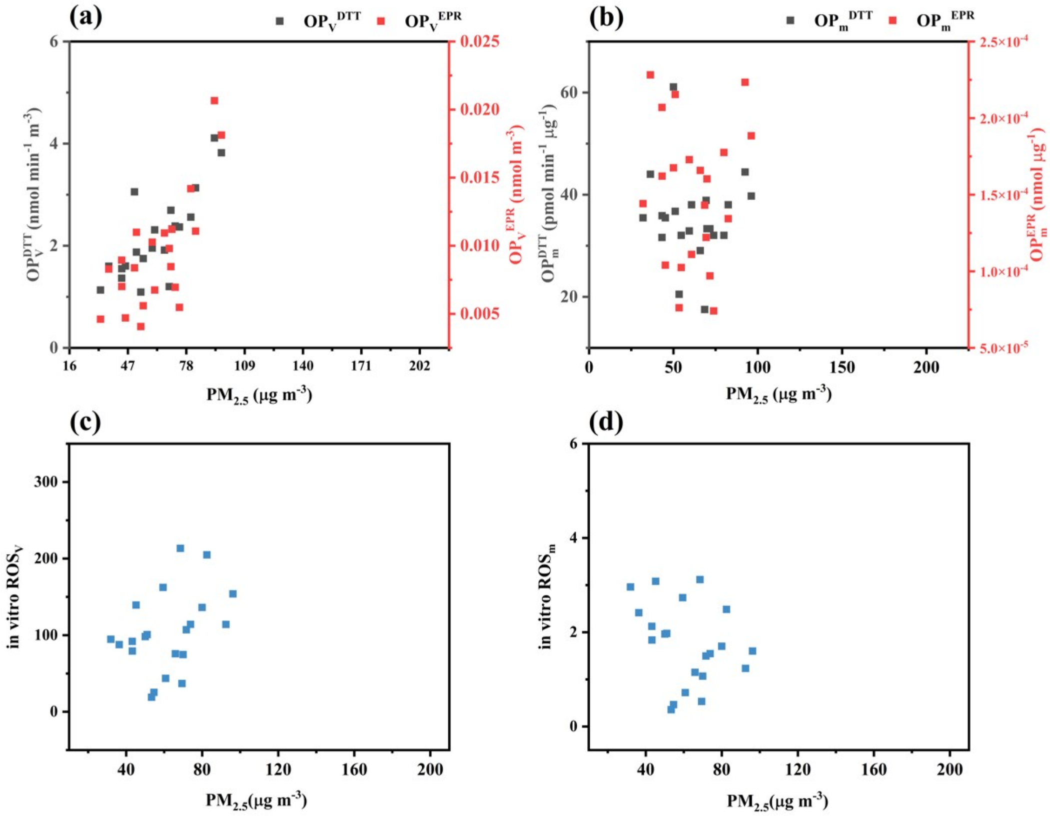

Figure S6. Correlation between (a) OP_v , (b) *in vitro* ROS_V, (c) OP_m and (d) *in vitro* ROS_m with $PM_{2.5}$ mass concentration in non-haze episodes, respectively.

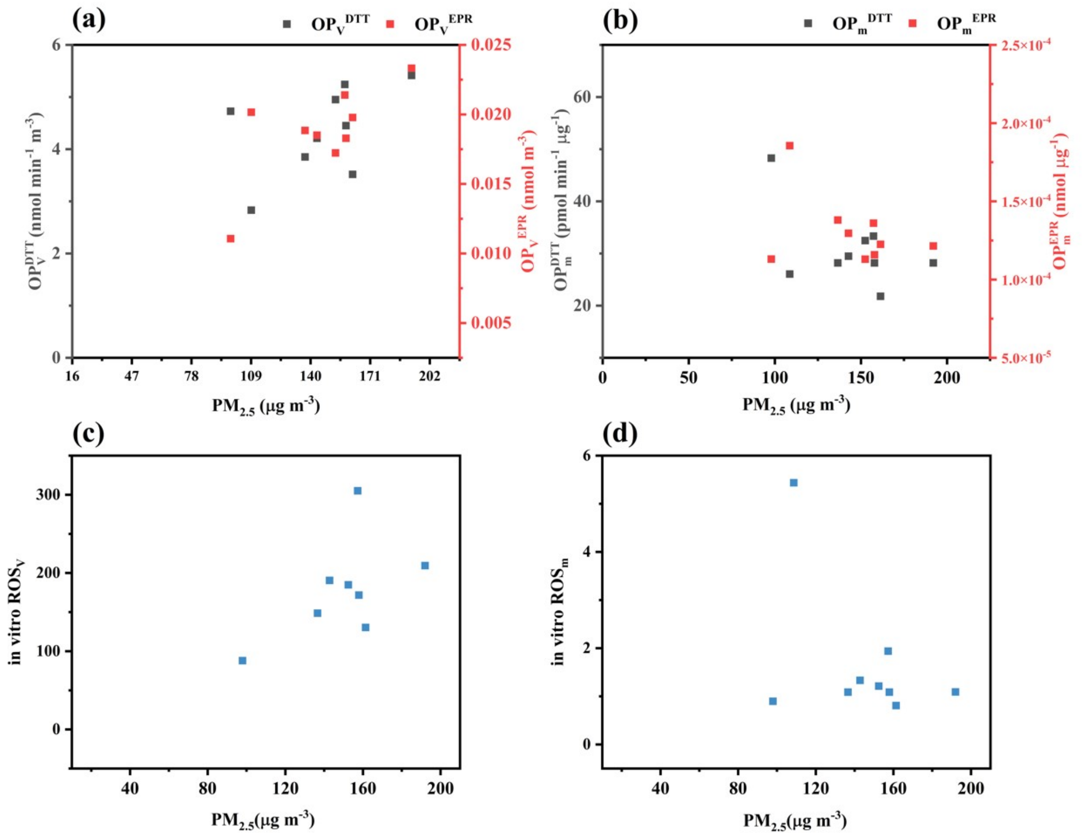

Figure S7. Correlation between (a) OP_v, (b) *in vitro* ROS_V, (c) OP_m and (d) *in vitro* ROS_m with $PM_{2.5}$ mass concentration in non-haze episodes, respectively.

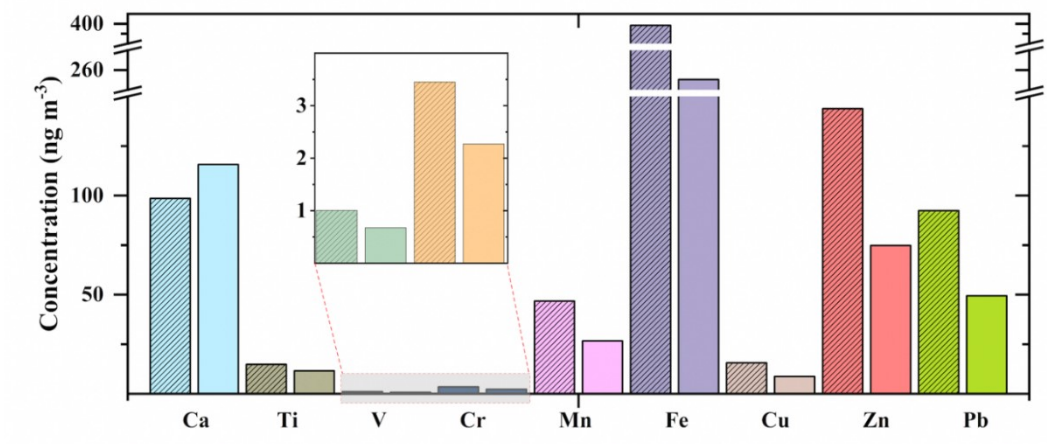

Figure S8. Comparison of metallic elements in $PM_{2.5}$ during haze (shadow) and non-haze period (unshadow) in Chongqing.

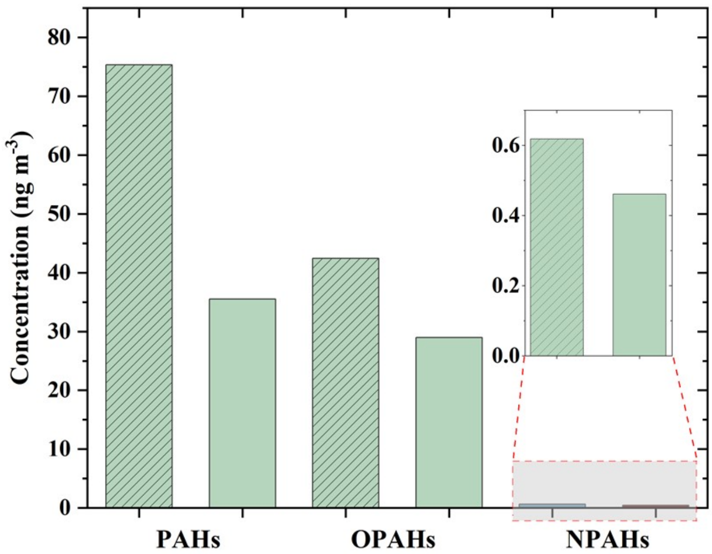

Figure S9. Comparison of PAHs, OPAHs, and NPAHs in $PM_{2.5}$ during haze (shadow) and non-haze period (unshadow) in Chongqing.

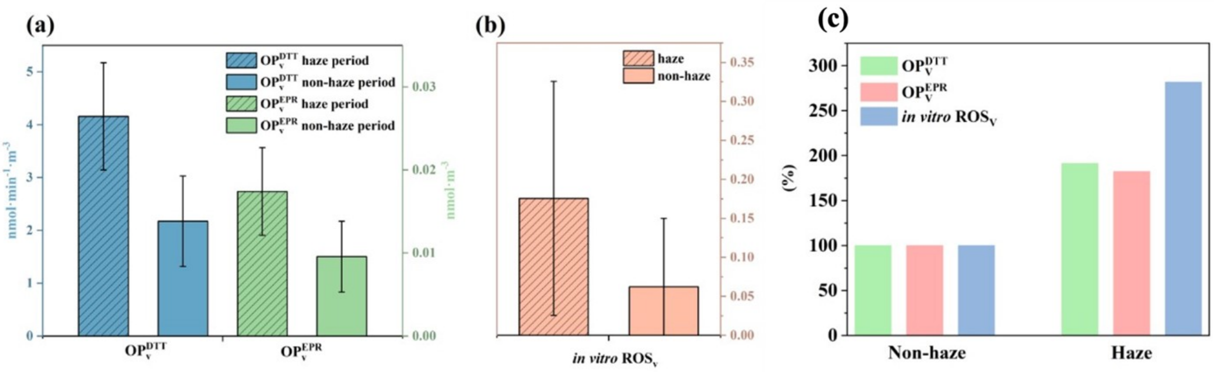

Figure S10. Comparison of (a) OP_V^{DTT}, OP_V^{EPR} and (b) *in vitro* ROS_V of $PM_{2.5}$ during haze (shadow) and non-haze period (unshadow) in Chongqing. (c) OP_V^{DTT}, OP_V^{EPR} and *in vitro* ROS_V during haze periods normalized to those measured during non-haze episodes.

References

1. J. C. Chow, J. G. Watson, L. W. A. Chen, W. P. Arnott, H. Moosmüller and K. Fung, Equivalence of elemental carbon by thermal/optical reflectance and transmittance with different temperature protocols, *Environ. Sci. Technol.*, 2004, **38**, 4414-4422.

2. J. C. Chow, J. G. Watson, J. Robles, X. Wang, L. W. A. Chen, D. L. Trimble, S. D. Kohl, R. J. Tropp and K. K. Fung, Quality assurance and quality control for thermal/optical analysis of aerosol samples for organic and elemental carbon, *Anal. Bioanal. Chem.*, 2011, **401**, 3141-3152.

3. J. C. Chow, J. G. Watson, L. W. A. Chen, M. C. O. Chang, N. F. Robinson, D. Trimble and S. Kohl, The IMPROVE_A Temperature Protocol for Thermal/Optical Carbon Analysis: Maintaining Consistency with a Long-Term Database, *J. Air Waste Manag. Assoc.*, 2007, **57**, 1014-1023.

4. EPA, Risk Assessment Guidance for Superfund (RAGS), Volume I Human Health Evaluation Manual (Part F, Supplemental Guidance for Inhalation Risk Assessment).*Journal*, 2009.

5. N. Galindo, E. Yubero, J. F. Nicolás, M. Varea and J. Crespo, Characterization of metals in PM_1 and PM_{10} and health risk evaluation at an urban site in the western Mediterranean, *Chemosphere*, 2018, **201**, 243-250.

6. H. Li, H. Wu, Q. g. Wang, M. Yang, F. Li, Y. Sun, X. Qian, J. Wang and C. Wang, Chemical partitioning of fine particle-bound metals on haze–fog and non-haze–fog days in Nanjing, China and its contribution to human health risks, *Atmos. Res.*, 2017, **183**, 142-150.

7. F. Li, J. Yan, Y. Wei, J. Zeng, X. Wang, X. Chen, C. Zhang, W. Li, M. Chen and G. Lü, $PM_{2.5}$-bound heavy metals from the major cities in China: Spatiotemporal distribution, fuzzy exposure assessment and health risk management, *J. Cleaner Prod.*, 2021, **286**, 124967.

8. J. Lv, M. Li, J. Xie, Z. Di, L. Zhao and R. Liu, Seasonal variation and chemical speciation analysis of $PM_{2.5}$ heavy Metals in Taiyuan City, *Environ. Sci. Technol.*, 2016, **39**, 126-131.

9. P. Pandey, D. K. Patel, A. H. Khan, S. C. Barman, R. C. Murthy and G. C. Kisku, Temporal distribution of fine particulates ($PM_{2.5}$, PM_{10}), potentially toxic metals, PAHs and Metal-bound carcinogenic risk in the population of Lucknow City, India, *J. Environ. Sci. Health A*, 2013, **48**, 730-745.

10. N. T. Hieu and B.-K. Lee, Characteristics of particulate matter and metals in the ambient air from a residential area in the largest industrial city in Korea, *Atmos. Res.*, 2010, **98**, 526-537.

11. Q. Liu, Z. Lu, Y. Xiong, F. Huang, J. Zhou and J. J. Schauer, Oxidative potential of ambient PM2.5 in Wuhan and its comparisons with eight areas of China, *Science of The Total*

Environment, 2020, **701**, 134844.

12. J. Wang, X. Lin, L. Lu, Y. Wu, H. Zhang, Q. Lv, W. Liu, Y. Zhang and S. Zhuang, Temporal variation of oxidative potential of water soluble components of ambient $PM_{2.5}$ measured by dithiothreitol (DTT) assay, *Sci. Total Environ.*, 2019, **649**, 969-978.

13. Y. Lyu, H. Guo, T. Cheng and X. Li, Particle Size Distributions of Oxidative Potential of Lung-Deposited Particles: Assessing Contributions from Quinones and Water-Soluble Metals, *Environ. Sci. Technol.*, 2018, **52**, 6592-6600.

14. J.-M. Li, S.-M. Zhao, S.-H. Xiao, X. Li, S.-P. Wu, J. Zhang and J. J. Schwab, Source apportionment of water-soluble oxidative potential of $PM_{2.5}$ in a port city of Xiamen, Southeast China, *Atmos. Environ.*, 2023, **314**, 120122.

15. Y. Yu, P. Cheng, Y. Li, J. Gu, Y. Gong, B. Han, W. Yang, J. Sun, C. Wu, W. Song and M. Li, The association of chemical composition particularly the heavy metals with the oxidative potential of ambient $PM_{2.5}$ in a megacity (Guangzhou) of southern China, *Environ. Res.*, 2022, **213**, 113489.

16. W. Liu, Y. Xu, W. Liu, Q. Liu, S. Yu, Y. Liu, X. Wang and S. Tao, Oxidative potential of ambient $PM_{2.5}$ in the coastal cities of the Bohai Sea, northern China: Seasonal variation and source apportionment, *Environ. Pollut.*, 2018, **236**, 514-528.

17. L. Zhang, X. Hu, S. Chen, Y. Chen and H.-Z. Lian, Characterization and source apportionment of oxidative potential of ambient $PM_{2.5}$ in Nanjing, a megacity of Eastern China, *Environ. Pollut. Bioavailability*, 2023, **35**, 2175728.

18. F. Yang, C. Liu and H. Qian, Comparison of indoor and outdoor oxidative potential of $PM_{2.5}$: pollution levels, temporal patterns, and key constituents, *Environ. Int.*, 2021, **155**, 106684.

19. R. Li, C. Yan, Q. Meng, Y. Yue, W. Jiang, L. Yang, Y. Zhu, L. Xue, S. Gao, W. Liu, T. Chen and J. Meng, Key toxic components and sources affecting oxidative potential of atmospheric particulate matter using interpretable machine learning: Insights from fog episodes, *J. Hazard. Mater.*, 2024, **465**, 133175.

20. Q. Chen, M. Wang, Y. Wang, L. Zhang, Y. Li and Y. Han, Oxidative Potential of Water-Soluble Matter Associated with Chromophoric Substances in $PM_{2.5}$ over Xi'an, China, *Environ. Sci. Technol.*, 2019, **53**, 8574-8584.

21. D. Chirizzi, D. Cesari, M. R. Guascito, A. Dinoi, L. Giotta, A. Donateo and D. Contini, Influence of Saharan dust outbreaks and carbon content on oxidative potential of water-soluble fractions of $PM_{2.5}$ and PM_{10}, *Atmos. Environ.*, 2017, **163**, 1-8.

22. M. M. Shafer, J. D. C. Hemming, D. S. Antkiewicz and J. J. Schauer, Oxidative potential of size-fractionated atmospheric aerosol in urban and rural sites across Europe, *Faraday Discuss.*, 2016, **189**, 381-405.

23. S. Weichenthal, M. Shekarrizfard, A. Traub, R. Kulka, K. Al-Rijleh, S. Anowar, G. Evans and M. Hatzopoulou, Within-City Spatial Variations in Multiple Measures of PM2.5 Oxidative Potential in Toronto, Canada, *Environmental Science & Technology*, 2019, **53**, 2799-2810.

24. T. Fang, V. Verma, J. T. Bates, J. Abrams, M. Klein, M. J. Strickland, S. E. Sarnat, H. H. Chang, J. A. Mulholland, P. E. Tolbert, A. G. Russell and R. J. Weber, Oxidative potential of ambient water-soluble $PM_{2.5}$ in the southeastern United States: contrasts in sources and health associations between ascorbic acid (AA) and dithiothreitol (DTT) assays, *Atmos. Chem. Phys.*, 2016, **16**, 3865-3879.

25. R. Qian, S. Zhang, C. Peng, L. Zhang, F. Yang, M. Tian, R. Huang, Q. Wang, Q. Chen, X. Yao and Y. Chen, Characteristics and potential exposure risks of environmentally persistent free radicals in $PM_{2.5}$ in the three gorges reservoir area, Southwestern China, *Chemosphere*, 2020, **252**, 126425.

26. Q. Chen, M. Wang, Y. Wang, L. Zhang, J. Xue, H. Sun and Z. Mu, Rapid determination of environmentally persistent free radicals (EPFRs) in atmospheric particles with a quartz sheet-based approach using electron paramagnetic resonance (EPR) spectroscopy, *Atmos. Environ.*, 2018, **184**, 140-145.

27. Q. Chen, H. Sun, Z. Mu, Y. Wang, Y. Li, L. Zhang, M. Wang and Z. Zhang, Characteristics of environmentally persistent free radicals in $PM_{2.5}$: Concentrations, species and sources in Xi'an, Northwestern China, *Environ. Pollut.*, 2019, **247**, 18-26.

28. Q. Chen, H. Sun, M. Wang, Z. Mu, Y. Wang, Y. Li, Y. Wang, L. Zhang and Z. Zhang, Dominant Fraction of EPFRs from Nonsolvent-Extractable Organic Matter in Fine Particulates over Xi'an, China, *Environ. Sci. Technol.*, 2018, **52**, 9646-9655.

29. L. Wang, W. Zhao, P. Luo, Q. He, W. Zhang, C. Dong and Y. Zhang, Environmentally persistent free radicals in $PM_{2.5}$ from a typical Chinese industrial city during COVID-19 lockdown: The unexpected contamination level variation, *J. Environ. Sci.*, 2024, **135**, 424-432.

30. J. Ai, W. Qin, J. Chen, Y. Sun, Q. Yu, K. Xin, H. Huang, L. Zhang, M. Ahmad and X. Liu, Pollution characteristics and light-driven evolution of environmentally persistent free radicals in $PM_{2.5}$ in two typical northern cities of China, *J. Hazard. Mater.*, 2023, **454**, 131466.

31. Q. Chen, M. Wang, H. Sun, X. Wang, Y. Wang, Y. Li, L. Zhang and Z. Mu, Enhanced health risks from exposure to environmentally persistent free radicals and the oxidative stress of $PM_{2.5}$ from Asian dust storms in Erenhot, Zhangbei and Jinan, China, *Environ. Int.*, 2018, **121**, 260-268.

32. X. Guo, N. Zhang, X. Hu, Y. Huang, Z. Ding, Y. Chen and H.-z. Lian, Characteristics and potential inhalation exposure risks of $PM_{2.5}$–bound environmental persistent free radicals

in Nanjing, a mega–city in China, *Atmos. Environ.*, 2020, **224**, 117355.

33. A. Filippi, R. Sheu, T. Berkemeier, U. Pöschl, H. Tong and D. R. Gentner, Environmentally persistent free radicals in indoor particulate matter, dust, and on surfaces, *Environ. Sci.: Atmos.*, 2022, **2**, 128-136.

34. M. Ahmad, J. Chen, Q. Yu, M. Tariq Khan, S. Weqas Ali, A. Nawab, W. Phairuang and S. Panyametheekul, Characteristics and Risk Assessment of Environmentally Persistent Free Radicals (EPFRs) of $PM_{2.5}$ in Lahore, Pakistan, *Int. J. Environ. Res. Public Health*, 2023, **20**, 2384.